

Knockdown of *OsHox33*, a member of the class III homeodomain-leucine zipper gene family, accelerates leaf senescence in rice

LUAN WeiJiang^{1*}, SHEN Ao¹, JIN ZhiPing², SONG SuSheng³, LI ZhengLong¹
& SHA AiHua⁴

¹College of Life Sciences, Tianjin Key Laboratory of Animal and Plant Resistance, Tianjin Normal University, Tianjin 300387, China;

²Institute of Genetics and Developmental Biology, Chinese Academy of Sciences, Beijing 100101, China

³School of Life Science, Tsinghua University, Beijing 100084, China;

⁴Oil Crops Research Institute, Chinese Academy of Agricultural Sciences, Wuhan 430062, China

Received August 9, 2013; accepted September 26, 2013

The class III homeodomain-leucine zipper (HD-Zip III) gene family plays important roles in plant growth and development, including regulation of apical embryo patterning, embryonic shoot meristem formation, leaf polarity, vascular development, and meristem function, with a particularly crucial function in leaf development. Although HD-Zip III members are highly conserved in land plants, previous studies, such as genetic analyses based on multiple mutants in *Arabidopsis* and other plants, suggest that various HD-Zip III family genes have evolved with distinct functions and pleiotropic effects on plant growth and development. In this study, we analyzed a HD-Zip III member, *OsHox33*, and demonstrated that it plays an important role in age-dependent leaf senescence in rice. We constructed two specific RNAi vectors derived from the 5'-end region and 3'-UTR of *OsHox33* to knockdown its expression. Transgenic plants harboring either RNAi construct displayed similar phenotypes of precocious leaf senescence symptoms, suggesting that knockdown of *OsHox33* accelerates leaf senescence in rice. *pOsHox33::GUS* fusion expression and RT-PCR revealed that *OsHox33* is highly expressed in young organs, especially in young meristems such as shoot apical meristems, intercalary meristems, and young callus. In addition, real-time PCR indicated that *OsHox33* was more highly expressed in young leaves than in old leaves. To further investigate *OsHox33* function, we analyzed chloroplast ultrastructure in different-aged leaves of RNAi plants, and found that *OsHox33* knockdown accelerated chloroplast degradation, which is consistent with RNAi phenotypes. Finally, real-time PCR studies showed that *OsHox33* can regulate the expression of *GS1* and *GS2*, two senescence-associated genes. Taken together, the work presented here provides new insights into the function of HD-Zip III members in plants.

HD-Zip III, leaf senescence, rice

Citation: Luan W J, Shen A, Jin Z P, et al. Knockdown of *OsHox33*, a member of the class III homeodomain-leucine zipper gene family, accelerates leaf senescence in rice. *Sci China Life Sci*, 2013, 56: 1113–1123, doi: 10.1007/s11427-013-4565-2

In plants, leaf senescence is a process of programmed cell death and degeneration regulated by both internal gene networks and external environmental factors. By limiting growth, precocious leaf senescence may heavily reduce

yields in crops such as rice, wheat, and maize. Leaf senescence is an active and age-dependent degeneration process [1]. Degenerated products of cellular components of senescent leaves are relocated as nutrients to reproductive or younger organs [2]. Recent molecular genetic and reverse-genetic studies have revealed the regulatory frame-

*Corresponding author (email: lwjzsq@163.com)

work and molecular mechanisms associated with leaf senescence. During this process, many senescence-associated genes (*SAGs*) are up-regulated and highly expressed [3]. A recent microarray analysis has demonstrated that more than 1200 *SAGs* are up- or down-regulated during leaf senescence [4]. These *SAGs* mainly encode proteases, nucleases, lipases, and hydrolases involved in nutrient recycling, stress response, and transcriptional regulation. The functions of many *SAGs* are still unclear so far.

Leaf senescence is accompanied by changes in leaf color. The most significant phenotype is that plant leaves become yellow or “stay green”, or produces lesion spots due to hypersensitive response, which reflect chlorophyll degradation and the breakdown of chloroplasts [5,6]. Several genes, such as *NYC1*, *NYC3*, *NYC4*, *NYC1-LIKE* (*NOL*), *SGRs*, and *RLS1*, have recently been reported to be involved in chlorophyll degradation and chloroplast breakdown in rice [7–13]. In the complex regulatory network during leaf senescence, sugar signaling is thought to play an important role in the induction of leaf senescence. In *Arabidopsis*, *HXX1* cloned from glucose insensitive mutant *gin2* can regulate leaf senescence by altering sugar levels [14], with its overexpression accelerating leaf senescence through increases in sugar levels. Several leaf senescence-associated mutants displaying delayed or accelerated leaf senescence have provided a better understanding of the mechanisms of leaf senescence regulation. For example, AT-hook transcription factor *ORE7*, F-box protein *ORE9*, R-transferase *DLS1*, WRKY family members *WRKY53* and *WRKY6*, NAC family transcription factors *AtNAP* and *ORE1*, and a small auxin-up RNA gene, *SAUR36*, all serve as positive regulators to promote leaf senescence [15–23], while U-box E3 ubiquitin gene *SAUL1* and three autophagy genes, *AtAPG7*, *AtAPG9*, and *AtAPG18a*, act as negative regulators to delay leaf senescence [24–27]. *WRKY54* and *WRKY70* are recently shown to cooperate as negative regulators to delay leaf senescence in *Arabidopsis thaliana* [28].

The homeodomain (HD) superfamily, one of the largest transcription factor families, is found in all eukaryotic organisms. Members of this superfamily all contain a homeodomain motif with 60 conserved amino acid residues. The HD superfamily is divided into six subfamilies based on differences in DNA binding features, gene structure, and the presence of motifs such as leucine-zipper homeodomain (HD-Zip), plant homeodomain (PHD), Knotted-related homeobox (*KNOX*), Wuschel-related homeobox (*WOX*), zinc finger-associated homeodomain (ZF-HD), and Bell homeodomain (*BELL*) [29,30]. In plants, the HD superfamily plays key roles in various biological processes, such as response to environmental conditions, meristem regulation, pollen maturation, regulation of floral development, embryogenesis, shoot apical meristem initiation and maintenance, and determination of inflorescence architecture [30]. In particular, recent research has revealed that ZF-HD family members can regulate leaf senescence. *OsDOS* and

OsTZF1, two CCH-type zinc finger proteins, serve as negative regulators of leaf senescence in rice. Knockdown of these two genes can accelerate leaf senescence, whereas their overexpression delays leaf senescence [31,32]. The HD-Zip subfamily, characterized by the presence of a homeodomain and a leucine zipper domain, is the largest plant HD superfamily, and can be classified into four groups: HD-Zip I to HD-Zip IV. HD-Zips are involved in various developmental processes. For example, HD-Zip I members participate in abiotic stress and hormone responses [33–37]. HD-Zip II members are associated with light and auxin responses [38,39], and HD-Zip IV members are involved in organ development and architecture changes as well as epidermal cell differentiation [40–42].

In *Arabidopsis*, five members of the HD-Zip III group (*PHABULOSA* (*PHB*), *PHAVOLUTA* (*PHV*), *REVOLUTA* (*REV*), *CORONA* (*CAN*), and *AtHB8*) have partial redundant functions mainly involved in shoot apical meristem maintenance, establishment of bilateral symmetry, and differentiation of the leaf central-peripheral axis [43–46]. In addition, recent research has shown that miRNA165 and miRNA166 can negatively regulate expression of HD-Zip III members such as *PHB*, *PHV*, and *CNA*. Mutation of these two microRNAs gives rise to HD-Zip III gain-of-function phenotypes [47–50]. HD-ZIP III members also have an important role in promoting apical fate in early embryogenesis; in *Arabidopsis*, mutations in their miRNA165- and miRNA166-binding sites are able to restore apical fate in *tpl-1*, a topless mutant [51]. In this study, we analyzed the characteristics, function, and expression pattern of HD-Zip III member *OsHox33*, and investigated chloroplast ultrastructure in *OsHox33*-RNAi transgenic plants in detail. Our results demonstrate that knockdown of *OsHox33* can accelerate leaf senescence in rice.

1 Materials and methods

1.1 Plant materials

Rice varieties Zhonghua 11, Nipponbare (*Oryza sativa* L. ssp. *japonica*) and RNAi transgenic plants were used in this study. The RNAi transgenic plants were generated from Zhonghua 11 and Nipponbare using the *Agrobacterium*-mediated transformation method. Plants were grown in the experimental field of the Tianjin Agricultural Academy of Science, Tianjin, and in Sanya, Hainan Province, China.

1.2 The construction of RNAi expression vector and rice transformation

Two different RNAi expression vectors were constructed. For RNAi 3'-UTR construction, a specific DNA region containing the *OsHox33* 3'-UTR was amplified using the primers ISHD1 (5'-CACCATCCATGGTTTCCAG-3') and ISHD2 (5'-GGTAACTCAATGCCGATTGC-3'). The re-

sulting fragment was inserted into an empty pANDA35HK binary vector with hygromycin and kanamycin resistance using a pENTR directional TOPO cloning kit (Invitrogen, USA). For RNAi 5'-end construction, a forward partial sequence of the *OsHox33* 5'-UTR and first exon was amplified using gene-specific primers with *Sac* I and *Hind* III restriction sites incorporated: ISHD547F (5'-TGTC-gagctcTGAAGACCAGAGAGAAGACG-3') and ISHD-547R (5'-GAGAAagcttTGAGACTGACCTGCGATTTC-3') (restriction endonuclease recognition sites are underlined). A reverse partial sequence containing the *OsHox33* 5'-UTR, first exon, and first intron was amplified using gene-specific primers with *Sma* I and *Hind* III sites: ISHD827F (5'-TGTCcccggtTGAAGACCAGAGAGAAGACG-3') and ISHD827R (5'-TCCCaaagcttGAACCTTCTCGTCACCAATC-3'). Both PCR products were inserted into a pCAMBIA-UBI-GUS binary vector with hygromycin resistance to obtain the resultant vector pCAMBIA-UBI-RNAi-*OsHox33*. Two empty binary vectors and the two resultant vectors were then introduced into wild-type plants using the *Agrobacterium*-mediated transformation procedure described by Hiei [61].

1.3 RT-PCR and real-time PCR analysis

For analysis of the expression of RNAi lines, RNAs were isolated from fresh, young (50-day-old) leaves using Trizol reagent (Invitrogen) and treated with DNase I (NEB, USA). For RT-PCR analysis of different organs, RNAs were similarly isolated from young fresh roots, mature leaves, stem apical meristems, mature panicles, and 0.5–3-cm long young panicles. cDNAs were synthesized from 1 µg total RNA using M-MLV reverse transcriptase (TaKaRa, Dalian, China). For real-time PCR analysis of leaves at different developmental stages, RNAs were isolated from young (30-day-old), mature (60-day-old), and old (86-day-old) leaves. One microliter of cDNA was used for RT-PCR analysis along with the gene-specific primers HDF (5'-CACACGCGACTTTTGGACT-3') and HDR (5'-GGAGATTTCATAGAGCGGTCG-3'). *OsActin1* was used as an internal control gene, with ActinF (5'-GACTCTGGTGATGGTGTCAGC-3') and ActinR (5'-GGCTGGAAGAGGACCTCAGG-3') as primers for gene amplification. *OsHox33* amplification conditions were as follows: 2 min at 95°C, followed by 35 cycles of 30 s at 94°C, then 30 s at 59°C, 30 s at 72°C, and a final extension for 5 min at 72°C. For *OsActin1*, the following conditions were used: 2 min at 95°C, followed by 25 cycles of 30 s at 94°C, then 30 s at 60°C, 30 s at 72°C, and a final step of 5 min at 72°C. Three replicates were carried out for each reaction. Real-time PCR was performed using 1 µL cDNA and SYBR Green PCR master mix (Tiangen, Beijing, China) in a MyiQ2 two-color real-time PCR detection system (Bio-Rad, USA). The $2^{-\Delta\Delta C_t}$ method described by Livak [62] was used for the analysis of relative gene expression. Three replicates of each reaction

were performed, and *OsActin1* was used as an internal control for relative quantification of target gene expression. The following primers were used: GS1F (5'-GCAGAACGCAAGGGCTACT-3'), GS1R (5'-ATGTCGTGGCGTCAAGAAGC-3'), GS2F (5'-TTCTGTCTGGGGATTGGTCT-3'), and GS2R (5'-GGACTCAAAATACAGACCCAG-3'). Amplification conditions were as follows: 2 min at 95°C, followed by 40 cycles of 20 s at 95°C, 30 s at 60°C, and 30 s at 68°C.

1.4 GUS expression assay

An approximately 2100-bp long portion of the *OsHox33* genomic sequence upstream from the putative start codon was amplified with *OsHox33* specific primers HDGUSF (5'-GCTCgaattcCAGATTGCTTCATCGTTTGC-3') and HDGUSR (5'-TACTctgcagCTCCTCGTCGCTGCTTGTAC-3'). The underlined bases are restriction endonuclease recognition sites. The amplified DNA fragment was inserted into a pCAMBIA 1308-GUS vector using the *Eco*R I and *Pst* I sites in-frame with the *GUS* reporter gene to produce the resultant vector pOsHox33::GUS. After sequencing confirmation, the vector was introduced into Nipponbare wild-type plants via *Agrobacterium*-mediated transformation [61]. Transgenic plants were confirmed by selection on hygromycin and PCR amplification. Transgenic rice tissues were collected and incubated in GUS staining solution (100 mmol L⁻¹ phosphate buffer (pH 7.0), 10 mmol L⁻¹ EDTA, 1 mmol L⁻¹ potassium ferricyanide, 0.1% Triton X-100, and 2 mmol L⁻¹ X-Gluc) overnight at 37°C. Samples were then washed with 70% ethanol and fixed in FAA (5% formaldehyde, 5% acetic acid, and 80% ethanol) for microscopic observation.

1.5 Transmission electron microscopy

Detached leaves from different leaf-age stages of RNAi 3'-UTR construct lines and corresponding empty vector transgenic lines were fixed in a solution of 2.5% glutaraldehyde in phosphate buffer (pH 7.2) for 4 h. The specimens were then rinsed and postfixed overnight in 1% OsO₄ fixation buffer. Specimens were treated and processed as previously described [5]. Finally, specimens were observed by transmission electron microscopy (Hitachi, Tokyo, Japan).

2 Results

2.1 HD-Zip III members and sequence analysis in rice

OsHox33 encodes a protein of 855 amino acid residues, and contains 18 exons and 17 introns based on analysis of complete cDNA and rice genomic sequences. The protein contains four domains: Homeodomain (Homeobox), the basic leucine-zipper domain (bZip), START domain, and MEKHLA domain (Figure 1A). Homeobox and bZip do-

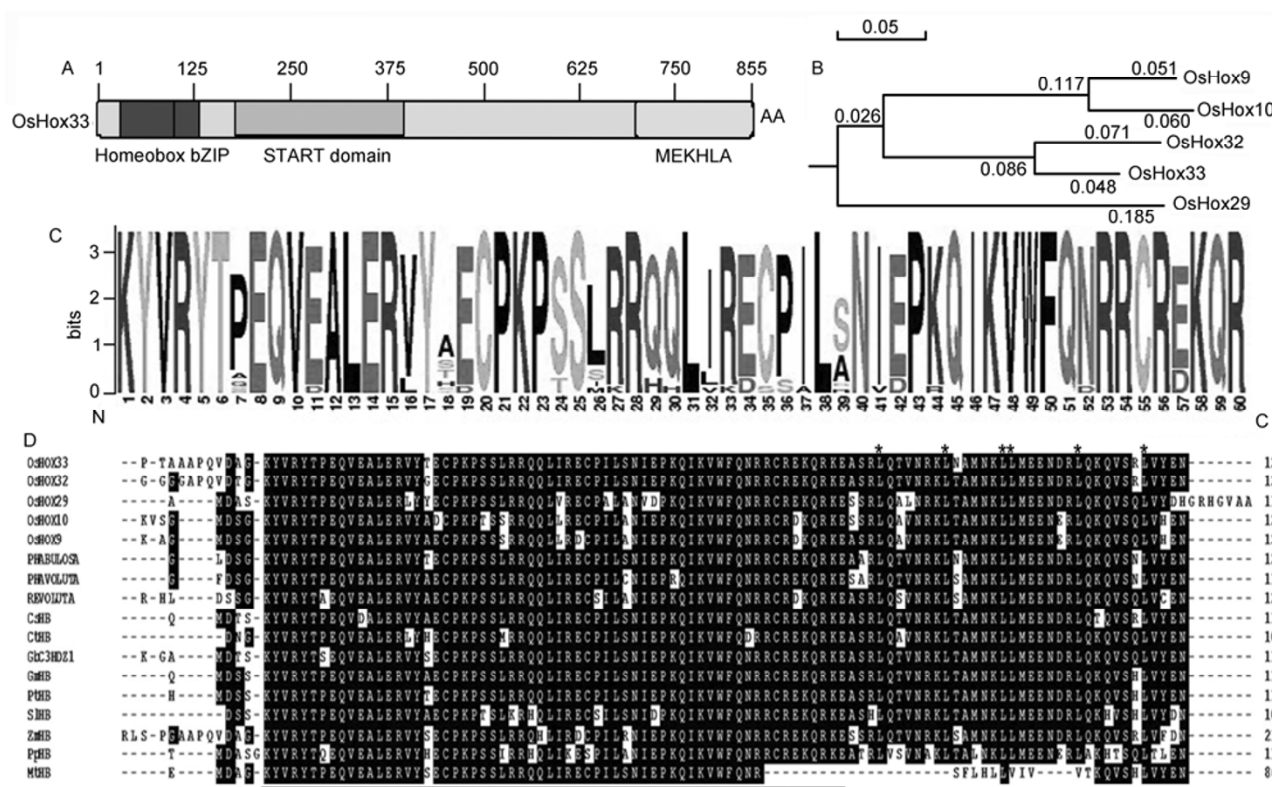


Figure 1 HD-Zip III members and sequence analysis in different species. A, Domain composition of the OsHox33 protein; AA stands for amino acid residues. *OsHox33* encodes a protein of 855 amino acid residues and contains four domains: Homeodomain (Homeobox), basic leucine-zipper (bZip), START, and MEKHLA domains. B, Phylogenetic tree of five rice HD-Zip III proteins. C, Conserved amino acid residues of the homeobox domain across 11 plant species: *Oryza sativa*, *Arabidopsis thaliana*, *Cucumis sativus*, *Citrus trifoliata*, *Ginkgo biloba*, *Glycine max*, *Populus trichocarpa*, *Solanum lycopersicum*, *Zea mays*, *Physcomitrella patens*, and *Medicago truncatula*. Degree of conservation of residues across all proteins is represented by the height of each letter; a position with all identical residues has a high bit score. The data were analyzed using WebLogo 3 software at <http://weblogo.berkeley.edu/>. D, Amino acid sequences of OsHox33 and other HD-ZIP members in different species identified by BLAST homology. Sequences were aligned using DNASTar software. The black line at the bottom indicates the conserved homeobox domain region; asterisks indicate the position of the six leucine residues in the Lxxxxxx-LxxxxxxLxxxxxxLxxxxxxL motif of the bZIP domain. Accession numbers of the corresponding member proteins in different species are OsHox33: NP_001067260; OsHox32: NP_001050745; OsHox9: Q9AV49; OsHox10: Q6TAQ6; OsHox29: Q5QM29; PHAVOLUTA (*Arabidopsis thaliana*): NP_174337.1; PHABULOSA (*Arabidopsis thaliana*): BAJ14107.1; REVOLUTA (*Arabidopsis thaliana*): AAF42938.1; PtHB: XP_002298892; PpHB: BAA92366; GmHB: XP_003546255; GbC3HDZ1, ABD75306; CshB: XP_004158070; MthB: XP_003594520; CthB: ACL51017; SIHB: XP_004233170; and ZmHB: DAA55130.

mainly are highly conserved in plants. The bZip domain contains a motif with six leucine residues, Lxxxxxx-LxxxxxxLxxxxxxLxxxxxxL (Figure 1D). Of the 60 amino acid residues in the homeobox, 38 are highly conserved in different plant species (Figure 1C). However, amino acid residues at some positions are quite variable, e.g., seven different amino acid residues, including Thr, Gly, Tyr, Ala, His, and Ser, are found at position 18 in 11 plant species (Figure 1C). In addition, amino acid residues at positions 17, 26, and 39 also vary greatly among different plant species. Five HD-Zip III proteins are encoded by the rice genome (*OsHox9*, *OsHox10*, *OsHox29*, *OsHox32*, and *OsHox33*), and are divided into three clades (Figure 1B). Based on amino acid similarities, clade 1 comprises *OsHox9* and *OsHox10*, and clade 2 consists of *OsHox32* and *OsHox33*. Because its amino acid sequence is different from those in clades 1 and 2, *OsHox29* is grouped separately as clade 3 (Figure 1B). In a phylogenetic tree of HD-Zip III members

from different plant species (Figure S1 in Supporting Information), *OsHox33* is most closely related to *ZmHB* in maize. *OsHox33*, *ZmHB*, and *OsHox32* group are in the same clade, which is distinct from the clade containing *PHABULOSA* and *PHAVOLUTA* from *Arabidopsis* (Figure S1). In addition, 11 of the 60 homeobox amino acid residues are variable among the five HD-Zip III members of rice (Figure 1D). Position 18 is particularly variable: Thr, Gly, and Tyr in *OsHox33*, *OsHox32*, and *OsHox29*, respectively, and Ala in *OsHox9* and *OsHox10*. *OsHox33* and *OsHox32* are surprisingly similar based on homeobox amino acid composition; only amino acid residue 18 is different between them (Figure 1D).

2.2 Knockdown of *OsHox33* accelerates leaf senescence in rice

To reveal the function of *OsHox33* in rice, we constructed

two RNAi vectors using specific fragments from the 3'-UTR or 5'-end region (5'-UTR and first exon) of *OsHox33*. These two RNAi constructs and two empty vectors were introduced into wild-type plants to produce transgenic plants. We obtained 47 T_0 transgenic plants of 16 independent lines with the RNAi 3'-UTR construct, and 61 transgenic plants of 23 independent lines with the RNAi 5'-end construct. We randomly selected 15 lines with the 5'-end RNAi construct and 10 lines with the 3'-UTR RNAi construct to obtain T_1 generation plants. Four of 15 lines with the 5'-end RNAi construct exhibited leaf senescence phenotypes. These plants initially displayed lesion spots in and around leaf midribs; the spots eventually expanded and increased throughout all parts of the leaves, leading to leaf wilting and death (Figure 2D and E). Two of 10 3'-UTR RNAi construct lines exhibited a similar but more severe phenotype: in addition to the appearance of lesion spots, yellowing occurred at leaf tips and spread to the rest of the leaf, leading to leaf wilting and death (Figure 2A–C). In contrast, two empty transgenic lines exhibited a normal phenotype, indicating that knockdown of *OsHox33* accelerated rice leaf senescence. To confirm the validity of the two RNAi constructs, we analyzed *OsHox33* expression in RNAi transgenic plants by RT-PCR. The result showed that the expression of *OsHox33* in RNAi transgenic plants with the phenotype of these two constructions was seriously reduced compared with that in two empty transgenic plants, suggesting that two RNAi constructions were efficient (Figure 2F). We also detected *OsHox33* expression in RNAi lines exhibiting normal phenotypes, but this expression was

similar to that observed in the two empty transgenic plants (data not shown). In addition, transgenic plants with the 3'-UTR RNAi construct were earlier to display the senescence phenotype, which was observed about 50 d after sowing. Heading date was also delayed in 3'-UTR RNAi lines, possibly as a result of the extreme leaf senescence (Figure 2C).

2.3 *OsHox33* expression patterns

To investigate *OsHox33* expression patterns, we constructed a fusion plasmid containing the *OsHox33* promoter region and a *GUS* reporter gene. This fusion vector, *pOsHox33::GUS*, was introduced into wild-type Nipponbare to generate transgenic plants. *GUS* staining was visible in different tissues and organs, such as young meristems, roots, stems, leaves, and panicles, and was strongest in young organs, including young callus, leaves, roots, meristems, and panicles (Figure 3A–J). In contrast, *GUS* staining was not observed in mature organs, such as old callus, old roots, and mature panicles. Extremely strong *GUS* expression was detected in young callus and intercalary meristems (Figure 3L and indicated by arrows in Figure 3E). Strong expression was also detected in young tiller tips (Figure 3K). In inflorescences, *GUS* expression varied among panicle developmental stages (Figure 3E–J). The strongest *GUS* expression was detected in 0.5-cm and 1.2-cm long young panicles (Figure 3E and F), with slightly reduced expression observed in 2–18-cm long young panicles (Figure 3G–J). Within panicles, *GUS* activity was mainly detected in glums and rachises; no *GUS* expression was observed in stamens

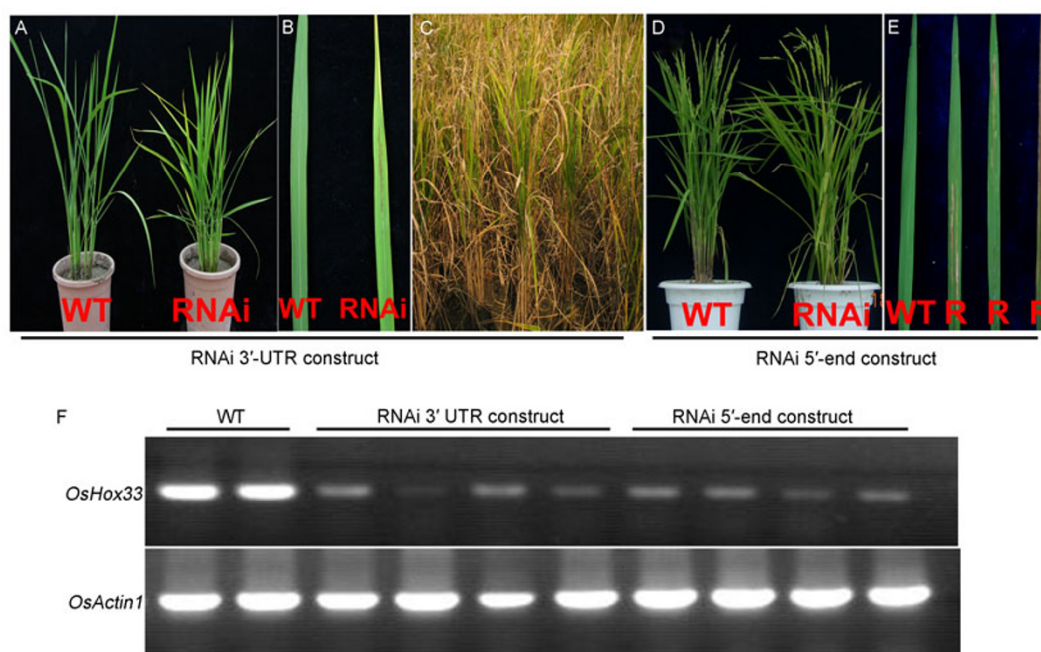


Figure 2 Phenotypes and expression analysis of *OsHox33* RNAi lines. A and B, Phenotypes of approximately 60-day-old transgenic plants harboring an *OsHox33* 3'-UTR fragment (RNAi) or the corresponding empty vector (WT). C, Phenotype of approximately 100-day-old RNAi 3'-UTR plants. D and E, Phenotypes of approximately 75-day-old transgenic plants harboring an *OsHox33* 5'-end fragment (RNAi) or the corresponding empty vector (WT). F, Results of RT-PCR analysis of RNAi and WT plants.

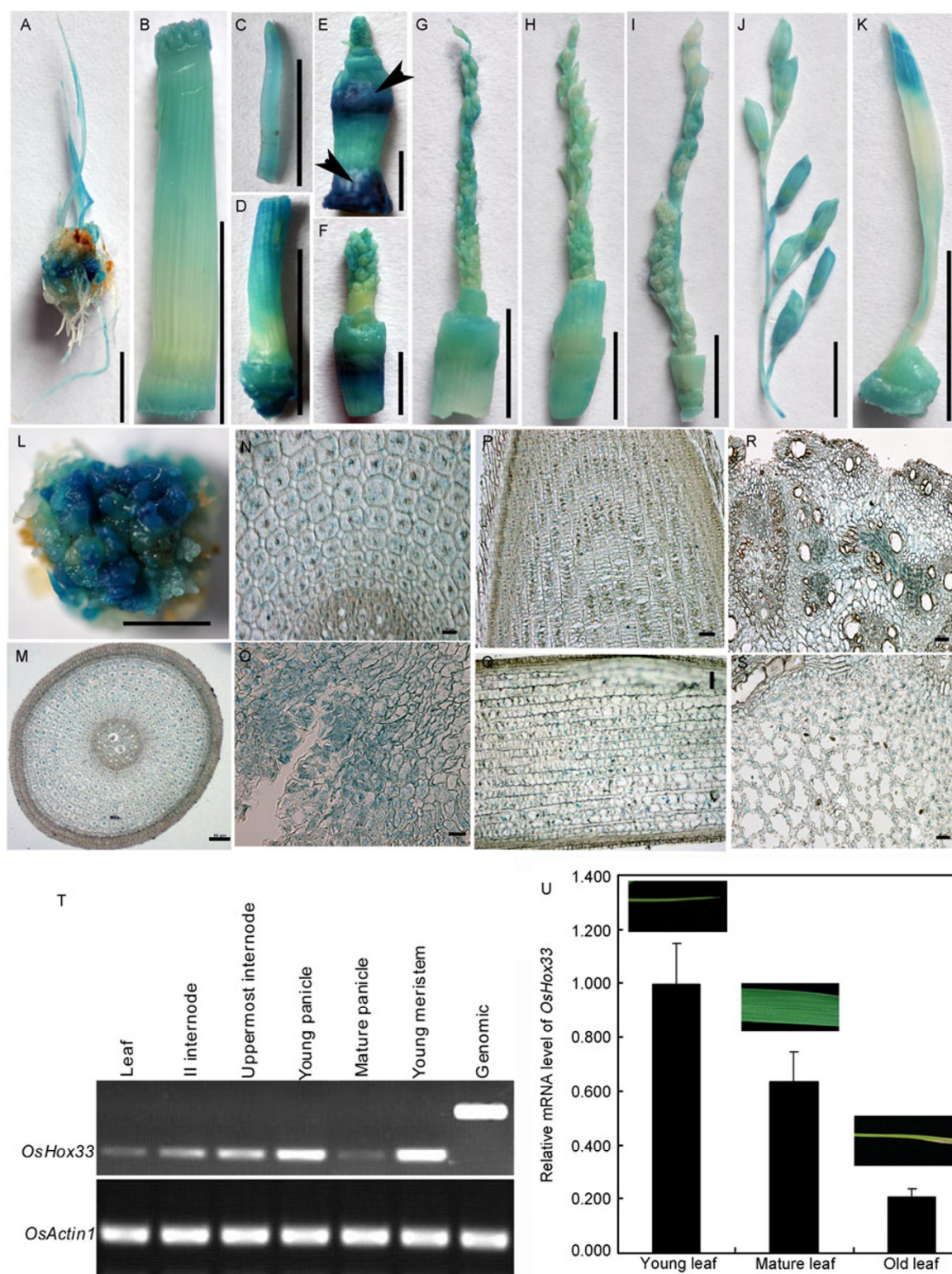


Figure 3 Expression analysis of *OsHox33*. A–S, *GUS* expression of *OsHox33* in different tissues and organs. A, Young leaves. B, Culm. C, Young roots. D, Young stem apical meristem. E–J, Different developmental stages of young panicle and intercalary meristem (indicated by arrows). E, 0.6-cm long panicle (the arrow indicates *GUS* expression in the intercalary meristem). F, 1.1-cm long young panicle. G, 2.3-cm long young panicle. H, 2.8-cm long young panicle. I, 3.5-cm long young panicle. J, Young panicle of the pollen-filling stage (18-cm long). K, Young tiller. L, Young callus. M and N, Cortex cells from cross sections of young roots; N is a magnified portion of M. O, Meristematic cells from longitudinal sections of young roots. P and Q, Cells of mitotic and elongation zones from longitudinal sections of young roots. R and S, Meristematic cells from longitudinal sections of the intercalary meristem; S is a magnified portion of R. T, Results of RT-PCR analysis of *OsHox33* in different rice organs. U, Results of real-time PCR analysis of *OsHox33* from different leaf stages. Scale bars: A–K, 1 cm; L, 1.5 mm; M–R, 50 μ m.

and stigmas (Figure 3J), suggesting that *OsHox33* may be mainly expressed in green organs. We also examined different tissue sections for *GUS* activity. In root cross sections, *GUS* expression was mainly detected in cortex cells (Figure 3M and N). *GUS* activity was also observed in mitotic and elongation zones in longitudinal sections (Figure 3P and Q), suggesting that *OsHox33* is primarily expressed in tissues undergoing active cell division. Furthermore, strong *GUS* expression was exhibited in callus meristem and intercalary meristem cells (Figure 3O, R, and S). To further investigate *OsHox33* expression in different organs, we isolated RNAs from mature leaves, various culms, shoot apical meristems, 0.5–3-cm long young panicles, and mature panicles, and used RT-PCR to analyze the expression of *OsHox33* in these organs. High *OsHox33* expression was detected in stem apical meristems and young panicles, whereas expression in mature panicles and leaves was low (Figure 3T). Finally, we investigated *OsHox33* expression during different stages of leaf development using real-time PCR; *OsHox33* expression was elevated in young leaves, with lower expression displayed in mature and old leaves (Figure 3U). These results are in agreement with the *GUS* expression analysis, indicating that *OsHox33* is mainly expressed in young organs and actively dividing cells, and may play crucial roles in rice growth and development.

2.4 Analysis of chloroplast ultrastructure in RNAi transgenic plants

We analyzed chloroplast ultrastructure at different leaf-age stages in RNAi transgenic plants and transgenic plants with

empty vectors (control plants). Chloroplast ultrastructure was obviously different between RNAi and empty vector lines (Figure 4). In young leaves of control plants, grana stacks were arranged in chloroplasts in a clear and regular fashion, with no accumulation of starch granules (Figure 4A and B). In contrast, the grana stack arrangement in RNAi-line chloroplasts was obscure and disordered, with many starch granules present (Figure 4C and D), suggesting accelerated chloroplast degradation. In old leaves of control plants, grana stacks were obscure and loose, with starch granules obvious (Figure 4E and F); in the RNAi lines, grana stacks in chloroplasts of old leaves completely disappeared, with obvious plastoglobuli and slightly shrunken chloroplasts observed (Figure 4G and H). These observations collectively indicate that *OsHox33* knockdown can accelerate leaf senescence in rice.

2.5 Expression analysis of senescence-associated genes in RNAi transgenic plants

To investigate senescence-associated gene expression in RNAi transgenic plants, we analyzed the expression of *GS1* and *GS2*, two senescence-related genes in rice. *GS1* and *GS2* display contrary expression patterns during rice leaf senescence: *GS1* expression was reduced, while *GS2* expression was increased. We observed that *GS1* expression was lower, and *GS2* expression was higher, in the two RNAi transgenic plants than in controls (Figure 5A and B), suggesting that *OsHox33* can regulate the expression of senescence-associated genes.

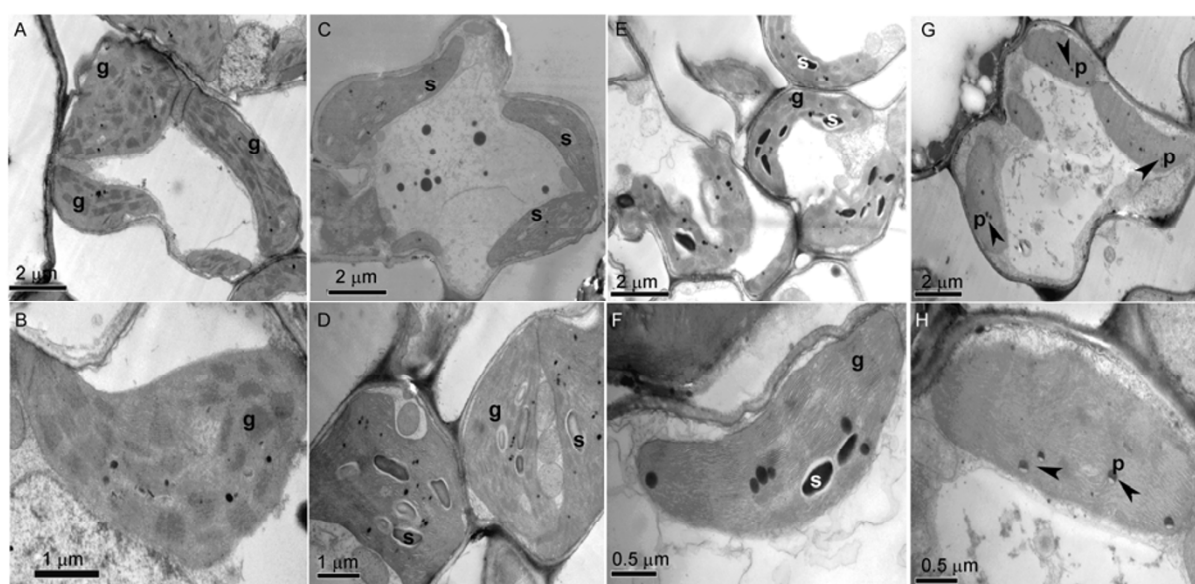


Figure 4 Chloroplast ultrastructure in different-aged leaves of RNAi lines. A and B, Young leaves of transgenic plants harboring the empty vector. C and D, Young leaves of RNAi plants. E and F, Old leaves of transgenic plants with empty vectors. G and H, Old leaves of RNAi plants. g, grana stack; p, plastoglobuli (indicated by arrow); s, starch granule.

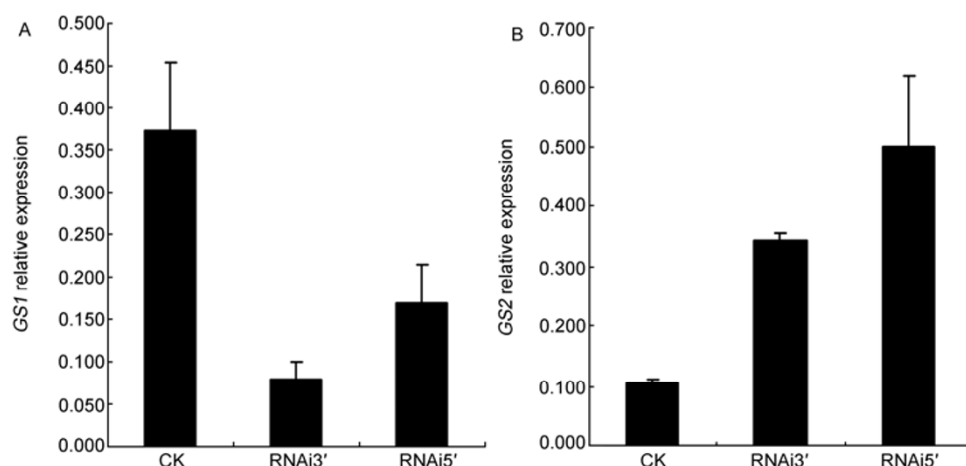


Figure 5 *GS1* and *GS2* expression in RNAi transgenic plants. Leaves were harvested from 50-day-old plants, and real-time PCR was carried out for analysis of (A) *GS1* and (B) *GS2* expression. RNAi3', RNAi5', and CK refer to transgenic plants with an RNAi 3'-UTR construct, RNAi 5'-end construct, and empty vector, respectively.

3 Discussion

3.1 Complex and diverse functions of HD-Zip III transcription factors in plants

In *Arabidopsis*, the HD-Zip III family, including PHB, PHV, REV, CNA and ATHB8, primarily regulates apical embryo patterning, embryonic shoot meristem formation, leaf polarity, vascular development, and meristem function [46]. Of these five members, PHB, PHV, and REV display overlapping and crucial roles during the establishment of apical bilateral symmetry and shoot apical meristems during embryogenesis. PHB and PHV also have significant functions in the initiation of postembryonic shoot apical meristem and floral meristem the and lateral organ patterning. The *REV* gene, the only HD-Zip III family member whose loss gives rise to a visible phenotype in a single mutant, is required for formation and initiation of lateral shoot meristems and floral meristems [52]. During meristem initiation, the *REV* protein exhibits elevated activity, whereas PHB and PHV show reduced activity, and CAN and ATHB8 are inactive [46,53]. CNA mainly regulates stem cell specification and organogenesis [54]. CNA and ATHB8 exhibit antagonistic functions toward PHB, PHV, and REV during lateral shoot meristem formation. In addition, ATHB8 plays a much less prominent role in embryo patterning. Furthermore, HD-Zip III transcription factors play a critical role in shade-induced hypocotyl elongation growth [55]. These previous studies provide evidence that HD-Zip III members have evolved distinct functions and exert different pleiotropic effects on growth and development in *Arabidopsis*.

HD-Zip III members are highly conserved in land plants, yet genetic analysis based on multiple mutants suggests significant functional differences among family members in *Arabidopsis* [53]. Functions of HD-Zip III members have also been studied in *Populus*, and have been found to differ from those observed in *Arabidopsis*. The *Populus* HD-Zip

III protein popREVOLUTA, orthologous to the REVOLUTA protein in *Arabidopsis*, plays an important regulatory role in cambium and secondary vascular tissue development, and influences cambium initiation and woody stem patterning [56]. Another *Populus* HD-Zip III, PtrHB7, plays a critical role in regulation of vascular cambium differentiation, as suppression of *PtrHB7* expression reduces xylem and increases phloem during secondary vascular differentiation [57]. In addition, heterologous expression in the *Arabidopsis revoluta* mutant of the HD-Zip III member *PpHB10* from the moss *Physcomitrella patens* resulted in uncoordinated stem growth [53]; *PpHB10* expression did not restore the *revoluta* phenotype [53], suggesting an independent and distinct evolution of *PpHB10*. These results indicate that HD-Zip III gene functions may differentiate and evolve in different plants.

Itoh et al. [58] analyzed expression patterns and ectopic expression phenotypes of five HD-Zip III members in rice, *OsHB1–OsHB5*. Their results indicated that these genes are essential for radial pattern formation during embryogenesis and shoot apical meristem establishment during leaf initiation. In this study, we have demonstrated that HD-Zip III family member *OsHox33*, which corresponds to *OsHB3*, plays an important role in age-dependent leaf senescence. Plants generated from two independent RNAi constructions displayed similar lesion-spot leaf senescence phenotypes. Our results indicate that *OsHox33* knockdown accelerates leaf senescence. In addition, *OsHox33* knockdown has a significant influence on chloroplast ultrastructure, revealing the functional importance of *OsHox33* in leaf chloroplasts, consistent with observed *OsHox33* RNAi-line phenotypes. In our study, GUS expression and RT-PCR revealed that *OsHox33* is highly expressed in shoot apical meristems and young organs, which is similar to expression patterns described in the study of Itoh et al. [58]. In their study, transgenic plants ectopically expressing *OsHB3* (*OsHox33*) did

not show morphologically abnormal phenotypes, whereas regenerated plants ectopically expressing microRNA166-resistant versions of the *OsHB3* gene exhibited severe defects, such as filamentous leaves and the ectopic production of leaf margins, shoots, and radialized leaves [58]. Although this result suggests that *OsHox33* plays important roles in leaf growth and development, no evidence of *OsHox33* RNAi was provided to elucidate the functions of *OsHox33* in their study. Because loss-of-function mutants are unavailable in rice, in contrast to *Arabidopsis*, we produced two specific RNAi constructs derived from the 5'-end region (5'-UTR and first exon) and 3'-UTR of *OsHox33* to reveal the function of *OsHox33*. Our results indicate that *OsHox33* can regulate the age-dependent senescence process. Taken together, these results provide a more comprehensive understanding of the functions of *OsHox33* in rice leaf growth and development.

3.2 The role of *OsHox33* in regulation of rice leaf senescence

Leaf senescence, an active and age-dependent degeneration process, is regulated by both internal gene networks and external environmental factors. Different types of genes and gene families play various roles in plant leaf senescence regulatory networks. For example, as reviewed in our introduction, AT-hook transcription factors, F-box proteins, WRKY transcription factors, NAC family transcription factors, and several autophagy genes act as positive or negative regulators to control leaf senescence. In addition, many genes can regulate leaf senescence by integrating phytohormone pathways and environmental factors. In soybean and *Arabidopsis*, senescence-associated receptor-like kinases can regulate leaf senescence by synergistic action of auxin and ethylene (ET) [59]. OsDOS (*Oryza sativa* delay of the onset of senescence), a CCCH-type zinc finger protein, is reportedly involved in the jasmonic acid (JA) regulatory pathway in leaf senescence. A genome-wide expression analysis revealed that many JA signaling-dependent genes were up-regulated in RNAi transgenic lines but down-regulated in overexpression transgenic lines, indicating that OsDOS acts as a negative regulator of leaf senescence by integrating the JA signaling pathway into age-dependent senescence [31]. The recently reported OsTZF1, a member of the CCCH-type zinc finger gene family, can delay leaf senescence in rice by regulating stress-related genes [32]. Moreover, several HD-Zip I proteins are also involved in hormone action or response to environmental stresses. *HAHB4*, a HD-Zip I protein, positively regulates JA and ET production during biotic stress and mechanical damage in sunflower. *HAHB4* overexpression up-regulates transcript levels of several genes involved in JA biosynthesis and defense-related processes such as the production of green leaf volatiles and trypsin protease inhibitors [37]. In *Arabidopsis*, HD-Zip I genes *ATHB6*,

ATHB7, and *ATHB12* are implicated in plant response to water deficit, as deduced from their transcriptional induction by water deficit conditions or abscisic acid (ABA) treatment [33,43,60]. In this study, we have demonstrated that a HD-Zip III member, *OsHox33*, can regulate leaf senescence in rice, but the underlying regulatory mechanism remains to be elucidated. To investigate whether *OsHox33* responds to phytohormone signaling or stress, we treated wild-type plants with drought stress, JA, ABA, and ET, and monitored *OsHox33* expression by real-time PCR. Compared with untreated controls, *OsHox33* expression was clearly reduced after treatment (data not shown), indicating that *OsHox33* mRNA levels are affected by environmental stress and phytohormones. We therefore speculate that *OsHox33* can regulate leaf senescence in rice by controlling stress-related genes and genes involved in the phytohormone signal transduction pathway. Although many genes related to leaf senescence have been identified, the regulatory network and interaction of these genes remain unclear. Investigations into the interaction of these identified genes will provide better insights into the leaf senescence regulatory network.

We thank Dr. Sheila McCormick (Plant Gene Expression Center, USDA/ARS and UC Berkeley) for editing assistance and advice, and Dr. Sheila A. Johnson-Brousseau (Plant Gene Expression Center, USDA/ARS and UC-Berkeley) for helpful discussions and advice. This work was supported by the National Natural Science Foundation of China (31171515), the Tianjin Natural Science Foundation of China (11JCZDJC17900), and the Knowledge Innovation and Training Program of Tianjin, Tianjin Municipal Education Commission (2013-1-2015-12).

- 1 Yoshida S. Molecular regulation of leaf senescence. *Curr Opin Plant Biol*, 2003, 6: 79–84
- 2 Himelblau E, Amasino M. Nutrients mobilized from leaves of *Arabidopsis thaliana* during leaf senescence. *J Plant Physiol*, 2001, 158: 1317–1323
- 3 Lohman K N, Gan S S, John M C, et al. Molecular analysis of natural senescence in *Arabidopsis thaliana*. *Plant Physiol*, 1994, 92: 322–328
- 4 van der Graaff E, Schwacke R, Schneider A, et al. Transcription analysis of *Arabidopsis* membrane transporters and hormone pathways during developmental and induced leaf senescence. *Plant Physiol*, 2006, 141: 776–792
- 5 Tanaka R, Hirashima M, Satoh S, et al. The *Arabidopsis*-accelerated cell death gene *ACD1* is involved in oxygenation of pheophorbide *a*: Inhibition of the pheophorbide *a* oxygenase activity does not lead to the “stay-green” phenotype in *Arabidopsis*. *Plant Cell Physiol*, 2003, 44: 1266–1274
- 6 Ren G, An K, Liao Y, et al. Identification of a novel chloroplast protein AtNYE1 regulating chlorophyll degradation during leaf senescence in *Arabidopsis*. *Plant Physiol*, 2007, 144: 1429–1441
- 7 Kusaba M, Ito H, Morita R, et al. Rice NON-YELLOW COLORING1 is involved in light-harvesting complex II and grana degradation during leaf senescence. *Plant Cell*, 2007, 19: 1362–1375
- 8 Jiang H, Li M, Liang N, et al. Molecular cloning and function analysis of the stay green gene in rice. *Plant J*, 2007, 52: 197–209
- 9 Park S Y, Yu J W, Park J S, et al. The senescence-induced staygreen protein regulates chlorophyll degradation. *Plant Cell*, 2007, 19: 1649–1664
- 10 Morita R, Sato Y, Masuda Y, et al. Defect in NON YELLOW COLORING 3, an α/β hydrolase-fold family protein, causes a stay

- green phenotype during leaf senescence in rice. *Plant J*, 2009, 59: 940–952
- 11 Sato Y, Morita R, Katsuma S, et al. Two short-chain dehydrogenase/reductases, NON-YELLOW COLORING 1 and NYC1-LIKE, are required for chlorophyll *b* and light-harvesting complex II degradation during senescence in rice. *Plant J*, 2009, 57: 120–131
 - 12 Jiao B B, Wang J J, Zhu X D, et al. A novel protein RLS1 with NB-ARM domains is involved in chloroplast degradation during leaf senescence in rice. *Mol Plant*, 2012, 5: 205–217
 - 13 Yamatani H, Sato Y, Masuda Y, et al. NYC4, the rice ortholog of *Arabidopsis* THF1, is involved in the degradation of chlorophyll-protein complexes during leaf senescence. *Plant J*, 2013, doi: 10.1111/tpj.12154
 - 14 Moore B, Zhou L, Rolland F, et al. Role of the *Arabidopsis* glucose sensor HXK1 in nutrient, light, and hormonal signaling. *Science*, 2003, 300: 332–336
 - 15 Hinderhofer K, Zentgraf U. Identification of a transcription factor specifically expressed at the onset of leaf senescence. *Planta*, 2001, 213: 469–473
 - 16 Woo H R, Chung K M, Park J H, et al. ORE9, an F-box protein that regulates leaf senescence in *Arabidopsis*. *Plant Cell*, 2001, 13: 1779–1790
 - 17 Yoshida S, Ito M, Nishida I, et al. Identification of a novel gene HYS1/CPR5 that has a repressive role in the induction of leaf senescence and pathogen-defence responses in *Arabidopsis thaliana*. *Plant J*, 2002, 29: 427–437
 - 18 Robatzek S, Somssich I E. Targets of AtWRKY6 regulation during plant senescence and pathogen defense. *Genes Dev*, 2002, 16: 1139–1149
 - 19 Miao Y, Laun T, Zimmermann P, et al. Targets of the WRKY53 transcription factor and its role during leaf senescence in *Arabidopsis*. *Plant Mol Biol*, 2004, 55: 853–867
 - 20 Guo Y, Gan S. AtNAP, a NAC family transcription factor, has an important role in leaf senescence. *Plant J*, 2006, 46: 601–612
 - 21 Lim P O, Kim Y, Breeze E, et al. Overexpression of a chromatin architecture-controlling AT-hook protein extends leaf longevity and increases the post-harvest storage life of plants. *Plant J*, 2007, 52: 1140–1153
 - 22 Kim J H, Woo H R, Kim J, et al. Trifurcate feed-forward regulation of age-dependent cell death involving miR164 in *Arabidopsis*. *Science*, 2009, 323: 1053–1057
 - 23 Hou K, Wu W, Gan S S. SAUR36, a small auxin up RNA gene, is involved in the promotion of leaf senescence in *Arabidopsis*. *Plant Physiol*, 2013, 161: 1002–1009
 - 24 Doelling J H, Walker J M, Friedman E M, et al. The APG8/12-activating enzyme APG7 is required for proper nutrient recycling and senescence in *Arabidopsis thaliana*. *J Biol Chem*, 2002, 277: 33105–33114
 - 25 Hanaoka H, Noda T, Yoshimoto K, et al. Leaf senescence and starvation-induced chlorosis are accelerated by the disruption of an *Arabidopsis* autophagy gene. *Plant Physiol*, 2002, 129: 1181–1193
 - 26 Xiong Y, Contento A L, Bassham D C. AtATG18a is required for the formation of autophagosomes during nutrient stress and senescence in *Arabidopsis thaliana*. *Plant J*, 2005, 42: 535–546
 - 27 Raab S, Drechsel G, Zarepour M, et al. Identification of a novel E3 ubiquitin ligase that is required for suppression of premature senescence in *Arabidopsis*. *Plant J*, 2009, 59: 39–51
 - 28 Besseau S, Li J, Palva E T. WRKY54 and WRKY70 co-operate as negative regulators of leaf senescence in *Arabidopsis thaliana*. *J Exp Bot*, 2012, 63: 2667–2679
 - 29 Ramachandran S, Hiratsuka K, Chua N H. Transcription factors in plant growth and development. *Curr Opin Genet Dev*, 1994, 4: 642–646
 - 30 Ariel F D, Manavella P A, Dezar C A, et al. The true story of the HD-Zip family. *Trends Plant Sci*, 2007, 12: 419–426
 - 31 Kong Z, Li M, Yang W, et al. A novel nuclear-localized CCCH-type zinc finger protein, OsDOS, is involved in delaying leaf senescence in rice (*Oryza sativa* L.). *Plant Physiol*, 2006, 141: 1376–1388
 - 32 Jan A, Maruyama K, Todaka D, et al. OsTZF1, a CCCH-tandem zinc finger protein, confers delayed senescence and stress tolerance in rice by regulating stress-related genes. *Plant Physiol*, 2013, 161: 1202–1216
 - 33 Söderman E, Mattsson J, Engström P. The *Arabidopsis* homeobox gene ATHB-7 is induced by water deficit and by abscisic acid. *Plant J*, 1996, 10: 375–381
 - 34 Söderman E, Hjällström M, Fahleson J, et al. The HD-Zip gene ATHB6 in *Arabidopsis* is expressed in developing leaves, roots and carpels and up-regulated by water deficit conditions. *Plant Mol Biol*, 1999, 40: 1073–1083
 - 35 Hanson J, Johannesson H, Engström P. Sugar-dependent alterations in cotyledon and leaf development in transgenic plants expressing the HDZip gene ATHB13. *Plant Mol Biol*, 2001, 45: 247–262
 - 36 Rueda E C, Dezar C A, Gonzalez D H, et al. Hahb-10, a sunflower homeobox-leucine zipper gene, is regulated by light quality and quantity, and promotes early flowering when expressed in *Arabidopsis*. *Plant Cell Physiol*, 2005, 46: 1954–1963
 - 37 Manavella P A, Arce A L, Dezar C A, et al. Cross-talk between ethylene and drought signalling pathways is mediated by the sunflower Hahb-4 transcription factor. *Plant J*, 2006, 48: 125–137
 - 38 Steindler C, Matteucci A, Sessa G, et al. Shade avoidance responses are mediated by the ATHB-2 HD-zip protein, a negative regulator of gene expression. *Development*, 1999, 126: 4235–4245
 - 39 Sawa S, Ohgishi M, Goda H, et al. The HAT2 gene, a member of the HD-Zip gene family, isolated as an auxin inducible gene by DNA microarray screening, affects auxin response in *Arabidopsis*. *Plant J*, 2002, 32: 1011–1022
 - 40 Abe M, Katsumata H, Komeda Y, et al. Regulation of shoot epidermal cell differentiation by a pair of homeodomain proteins in *Arabidopsis*. *Development*, 2003, 130: 635–643
 - 41 Ohashi-Ito K, Fukuda H. HD-zip III homeobox genes that include a novel member, ZeHB-13 (*Zinnia*)/ATHB-15 (*Arabidopsis*), are involved in procambium and xylem cell differentiation. *Plant Cell Physiol*, 2003, 44: 1350–1358
 - 42 Nakamura A, Nakajima N, Goda H, et al. *Arabidopsis* Aux/IAA genes are involved in brassinosteroid-mediated growth responses in a manner dependent on organ type. *Plant J*, 2006, 45: 193–205
 - 43 Baima S, Possenti M, Matteucci A, et al. The *Arabidopsis* ATHB-8 HD-zip protein acts as a differentiation-promoting transcription factor of the vascular meristems. *Plant Physiol*, 2001, 126: 643–655
 - 44 McConnell J R, Emery J, Eshed Y, et al. Role of PHABULOSA and PHAVOLUTA in determining radial patterning in shoots. *Nature*, 2001, 411: 709–713
 - 45 Emery J F, Floyd S K, Alvarez J, et al. Radial patterning of *Arabidopsis* shoots by class III HD-ZIP and KANADI genes. *Curr Biol*, 2003, 13: 1768–1774
 - 46 Prigge M J, Otsuga D, Alonso J M, et al. Class III homeodomain-leucine zipper gene family members have overlapping, antagonistic, and distinct roles in *Arabidopsis* development. *Plant Cell*, 2005, 17: 61–76
 - 47 Mallory A C, Reinhart B J, Jones-Rhoades M W, et al. microRNA control of PHABULOSA in leaf development: Importance of pairing to the microRNA 5' region. *EMBO J*, 2004, 23: 3356–3364
 - 48 Kim J, Jung J H, Reyes J L, et al. microRNA-directed cleavage of ATHB15 mRNA regulates vascular development in *Arabidopsis* inflorescence stems. *Plant J*, 2005, 42: 84–94
 - 49 Williams L, Grigg S P, Xie M, et al. Regulation of *Arabidopsis* shoot apical meristem and lateral organ formation by microRNA miR166g and its AtHD-ZIP target genes. *Development*, 2005, 132: 3657–3668
 - 50 Mallory A C, Vaucheret H. Functions of microRNAs and related small RNAs in plants. *Nat Genet*, 2006, 38: S31–S36
 - 51 Smith Z R, Long J A. Control of *Arabidopsis* apical-basal embryo polarity by antagonistic transcription factors. *Nature*, 2010, 464: 423–426
 - 52 Otsuga D, Deguzman B, Prigge M, et al. REVOLUTA regulates meristem initiation at lateral positions. *Plant J*, 2001, 25: 223–236

- 53 Prigge M J, Clark S E. Evolution of the class III HD-Zip gene family in land plants. *Evol Dev*, 2006, 8: 350–361
- 54 Green K A, Prigge M J, Katzman R B, et al. CORONA, a member of the class III homeodomain leucine zipper gene family in *Arabidopsis*, regulates stem cell specification and organogenesis. *Plant Cell*, 2005, 17: 691–704
- 55 Brandt R, Salla-Martret M, Bou-Torrent J, et al. Genome-wide binding-site analysis of REVOLUTA reveals a link between leaf patterning and light-mediated growth responses. *Plant J*, 2012, 72: 31–42
- 56 Robischon M, Du J, Miura E, et al. The *Populus* class III HD ZIP, popREVOLUTA, influences cambium initiation and patterning of woody stems. *Plant Physio*, 2011, 155: 1214–1225
- 57 Zhu Y, Song D, Sun J, et al. PtrHB7, a class III HD-Zip gene, plays a critical role in regulation of vascular cambium differentiation in *Populus*. *Mol Plant*, 2013, 6: 1331–1343
- 58 Itoh J, Hibara K, Sato Y, et al. Developmental role and auxin responsiveness of Class III homeodomain leucine zipper gene family members in rice. *Plant physiol*, 2008, 147: 1960–1975
- 59 Xu F, Meng T, Li P, et al. A soybean dual-specificity kinase, GmSARK, and its *Arabidopsis* homolog, AtSARK, regulate leaf senescence through synergistic actions of auxin and ethylene. *Plant Physiol*, 2011, 157: 2131–2153
- 60 Olsson A S, Engström P, Söderman E. The homeobox genes ATHB12 and ATHB7 encode potential regulators of growth in response to water deficit in *Arabidopsis*. *Plant Mol Biol*, 2004, 55: 663–677
- 61 Hiei Y, Ohta S, Komari T, et al. Efficient transformation of rice (*Oryza sativa* L.) mediated by *Agrobacterium* and sequence analysis of the boundaries of the T-DNA. *Plant J*, 1994, 6: 271–282
- 62 Livak K J, Schmittgen T D. Analysis of relative gene expression data using real-time quantitative PCR and the $2^{-\Delta\Delta C_t}$ method. *Methods*, 2001, 25: 402–408

Open Access This article is distributed under the terms of the Creative Commons Attribution License which permits any use, distribution, and reproduction in any medium, provided the original author(s) and source are credited.

Supporting Information

Figure S1 Phylogenetic tree of 17 HD-Zip III proteins from 11 plant species: *Oryza sativa* (Os), *Arabidopsis thaliana* (AT), *Cucumis sativus* (Cs), *Citrus trifoliata* (Ct), *Ginkgo biloba* (Gb), *Glycine max* (Gm), *Populus trichocarpa* (Pt), *Solanum lycopersicum* (Sl), *Zea mays* (Zm), *Physcomitrella patens* (Pp), and *Medicago truncatula* (Mt). Accession numbers of protein sequences are OsHox33: NP_001067260; OsHox32: NP_001050745; OsHox9: Q9AV49; OsHox10: Q6TAQ6; OsHox29: Q5QMZ9; PHAVOLUTA (*Arabidopsis thaliana*): NP_174337.1; PHABULOSA (*Arabidopsis thaliana*): BAJ14107.1; REVOLUTA (*Arabidopsis thaliana*): AAF42938.1; PtHB: XP_002298892; PpHB: BAA92366; GmHB: XP_003546255; GbC3HDZ1, ABD75306; CsHB: XP_004158070; MtHB: XP_003594520; CtHB: ACL51017; SlHB: XP_004233170; and ZmHB: DAA55130.

The supporting information is available online at life.scichina.com and www.springerlink.com. The supporting materials are published as submitted, without typesetting or editing. The responsibility for scientific accuracy and content remains entirely with the authors.